online data

Characterization of *Medicago truncatula* (barrel medic) hydroperoxide lyase (CYP74C3), a water-soluble detergent-free cytochrome P450 monomer whose biological activity is defined by monomer–micelle association

Richard K. HUGHES*[1], Eric J. BELFIELD*, Mylrajan MUTHUSAMAY*, Anuja KHAN†, Arthur ROWE†, Stephen E. HARDING†, Shirley A. FAIRHURST*, Stephen BORNEMANN*, Ruth ASHTON*, Roger N. F. THORNELEY* and Rod CASEY*

*John Innes Centre, Norwich Research Park, Norwich NR4 7UH, U.K., and †National Centre for Macromolecular Hydrodynamics, School of Biosciences, University of Nottingham, Sutton Bonington, Loughborough LE12 5RD, U.K.

We describe the detailed biochemical characterization of CYP74C3 (cytochrome P450 subfamily 74C3), a recombinant plant cytochrome P450 enzyme with HPL (hydroperoxide lyase) activity from *Medicago truncatula* (barrel medic). Steady-state kinetic parameters, substrate and product specificities, RZ (Reinheitszahl or purity index), molar absorption coefficient, haem content, and new ligands for an HPL are reported. We show on the basis of gel filtration, sedimentation velocity (sedimentation coefficient distribution) and sedimentation equilibrium (molecular mass) analyses that CYP74C3 has low enzyme activity as a detergent-free, water-soluble, monomer. The enzyme activity can be completely restored by re-activation with detergent micelles, but not detergent monomers. Corresponding changes in the spin state equilibrium, and probably co-ordination of the haem iron, are novel for cytochrome P450 enzymes and suggest that detergent micelles have a subtle effect on protein conformation, rather than substrate presentation, which is sufficient to improve substrate binding and catalytic-centre activity by an order of magnitude. The k_{cat}/K_m of up to 1.6×10^8 $M^{-1} \cdot s^{-1}$ is among the highest recorded, which is remarkable for an enzyme whose reaction mechanism involves the scission of a C–C bond. We carried out both kinetic and biophysical studies to demonstrate that this effect is a result of the formation of a complex between a protein monomer and a single detergent micelle. Association with a detergent micelle rather than oligomeric state represents a new mechanism of activation for membrane-associated cytochrome P450 enzymes. Highly concentrated and monodispersed samples of detergent-free CYP74C3 protein may be well suited for the purposes of crystallization and structural resolution of the first plant cytochrome P450 enzyme.

Key words: cytochrome P450, haem, hydroperoxide, metabolism, micelle, oxylipin.

INTRODUCTION

Cytochrome P450 enzymes are widespread in Nature, but members of the CYP74 (cytochrome P450 subfamily 74) subfamily of these enzymes, which are common in plants, have not been studied extensively. CYP74 enzymes are very different from other cytochrome P450 enzymes, for example CYP73 plant enzymes like cinnamate hydroxylases [1], or classical cytochrome P450 enzymes of microbial [2] or mammalian [3] origin, in that they have an atypical reaction mechanism that requires neither oxygen nor an NADPH-reductase [4], and as a consequence have extraordinarily high catalytic-centre activity. In this sense, they have more in common with non-classical mammalian cytochrome P450 enzymes like thromboxane synthase [5]. HPL (hydroperoxide lyase), or hemiacetal synthase [6], is a member of this CYP74 subfamily and has an important role in oxylipin metabolism, plant defence and the food industry [7,8]. The enzyme cleaves hydroperoxides, formed from the oxygenation of polyunsaturated fatty acids by the action of LOX (lipoxygenase), into an array of volatile and non-volatile products that have both antibacterial and organoleptic properties [7]. HPL has the same substrate specificity as another class of CYP74 enzymes, AOS (allene oxide synthase), which has been studied in much greater detail [9]. Unlike HPL, which cleaves hydroperoxides, AOS transforms them into unstable fatty acid epoxides; the mammalian equivalent of AOS is prostaglandin endoperoxide H synthase [10], but there is no known mammalian equivalent of HPL. The molecular mechanisms and primary determinants of this difference in specificity are unknown, primarily because there is no detailed structural and kinetic analysis of any homogeneously purified recombinant HPL. Structural and kinetic analyses of eukaryotic cytochrome P450 enzymes are especially problematic because they are: (i) membrane- or microsomal-associated with a surface hydrophobic domain, usually located at the N-terminus of the protein [1,11,12]; (ii) highly insoluble in the absence of detergents, and/or form a heterogeneous mixture of higher oligomers [13,14]; (iii) often studied using crude extracts and not as homogeneous, well-characterized, recombinant enzymes; (iv) poorly expressed in *Escherichia coli* and require engineering at their N-terminus to enhance water solubility which means that the heterologously expressed protein is not always biologically identical with the protein predicted from the cDNA; some N-terminal truncated cytochrome P450 enzymes, for example, interacted differently with their reductase and exhibited changes in specific activity and

Abbreviations used: AOS, allene oxide synthase; BCA, bicinchoninic acid; BI, benzimidazole; c.m.c., critical micellar concentration; CYP74, cytochrome P450 subfamily 74; DMPhP, dimethylphenylphosphine; Emulphogene, polyoxyethylene 10 tridecyl ether; EST, expressed sequence tag; HPL, hydroperoxide lyase; 9-HPODE, 9-*S*-hydroperoxyoctadeca-10*E*,12*Z*-dienoic acid; 13-HPODE, 13(S)-hydroperoxyoctadeca-(9*Z*,11*E*)-dienoic acid; 9-HPOTE, 9-*S*-hydroperoxyoctadeca-10*E*,12*Z*,15*Z*-trienoic acid; 13-HPOTE, 13-*S*-hydroperoxyoctadeca-9*Z*,11*E*,15*Z*-trienoic acid; IMAC, immobilized metal-ion affinity chromatography; ISD, in-source decay; LOX, lipoxygenase; MALDI–TOF, matrix-assisted laser-desorption ionization–time-of-flight; RZ, Reinheitszahl (or purity index); TMS, trimethylsilyl.

[1] To whom correspondence should be addressed (email richard.hughes@bbsrc.ac.uk).

product specificity; (v) relatively unstable and cannot be stored long term; and (vi) of uncertain oligomeric status in relation to the active species *in vitro*. All HPLs are membrane-associated and require detergent for extraction and solubilization. It has been difficult to resolve detergent and protein interactions, and consequently there is some disagreement about the oligomeric state of HPL purified from a number of higher plants, including guava fruit [15], bell pepper fruits [16,17], sunflower hypocotyls [18], apple fruits [19], tomato leaves [20] and fruits [21], soya bean seedlings [22] and watermelon [23]. The enzyme has been reported to be either trimeric or tetrameric; the oligomeric state of various recombinant HPLs: CYP74B1 [24], CYP74B2 [25], CYP74B3 [26], CYP74B4 [13], CYP74B5 [15], CYP74C1 [27] and CYP74C2 [28], and the effects of detergent removal, are hardly ever reported. The effects of detergent on increasing the activity of HPL are well documented (see [29]) but the molecular mechanism responsible for this activation is unknown.

There are currently no examples of a detailed biochemical characterization of any HPL. Homology modelling of HPL is difficult, due to very poor sequence identity with any other cytochrome P450 enzyme whose structure has been solved, unrecognizable protein folds, and the absence of structures for HPLs, or any other plant cytochrome P450. The structure of the AOS domain of the coral AOS–LOX chimaera has recently been solved and shown to be very similar to a catalase [9], but this is highly dissimilar to HPLs that are neither water-soluble nor predicted to have a catalase-fold. The structures of a number of water-soluble microbial cytochrome P450 enzymes have been solved [3], but those from eukaryotes – for example CYP2B4 [30], CYP2C5 [3], CYP2C8 [31], CYP2C9 [32], CYP3A4 [33] or CYP2A6 [34] – tend to have surface features for membrane interactions, and, to obtain crystals, required modifications in protein sequence to improve their water solubility and oligomeric state in the absence of detergents. All these are also highly dissimilar to any HPL and there remains a clear requirement for a detailed structural and kinetic analysis of HPL and of membrane-associated plant cytochrome P450 enzymes in general.

We first describe a procedure to obtain milligram quantities of a recombinant HPL from *Medicago truncatula* (barrel medic), herein classified as CYP74C3, and carry out a detailed biochemical characterization of CYP74C3 when isolated as a detergent-free protein with low activity. Secondly, we report the results of a comprehensive ligand-binding study. Thirdly, we examine the effects of detergent or substrate on re-activating the detergent-free enzyme, and distinguish between effects of substrate presentation and protein conformation. Detergent and substrate-induced changes in the spin state equilibrium of the haem iron, and their associated effects on haem co-ordination, are also reported. Comparisons are then made with other CYP74 and two mammalian membrane-associated cytochrome P450 enzymes as a basis to help improve our understanding of the differences in the regulation of catalysis of CYP74 and classical cytochrome P450 enzymes. Finally, the role of micellar-association and oligomeric status in defining CYP74C3 activity is discussed.

EXPERIMENTAL

Cloning and expression

CYP74C3 cDNA [full-length EST (expressed sequence tag) clone obtained from the Samuel Roberts Noble Foundation, Ardmore, OK, U.S.A.] was cloned into the destination vector pDEST17 using Gateway® technology (Invitrogen, Paisley, Scotland, U.K.) according to the manufacturer's instructions to give the plasmid pDEST17HPL-F + 7. Expression of CYP74C3 protein in pDEST17HPL-F + 7 occurred from the ATG start codon in pDEST17, so the encoded protein had a 22-N-terminal-amino-acid extension sequence (including a 6× N-terminal His tag and the peptide encoded by the Gateway® recombination *att* sequence). To determine whether this N-terminal sequence affected the oligomeric state [35] or kinetic properties of the expressed protein, the cDNA was also cloned into pDEST14 to give the plasmid pDEST14HPL-F + 8 for expression of the untagged protein. To investigate the role, if any, of a putative membrane targeting or pro-enzymic N-terminal sequence of CYP74C3, the cDNA was also cloned in pDEST14 to give the plasmid pDEST14HPL-F-8 and expressed without the first 11 amino acids (MASSSETSSTN) at the N-terminus.

Extraction and purification

His-tagged CYP74C3

Cultures [20 × 2 litre conical flasks each containing 1 litre of LB-G (Luria–Bertani medium without glucose) and 50 μg/ml ampicillin] of *E. coli* strain BL21(DE3) transformed with expression plasmid were grown at 37 °C to A_{600} (absorbance) of 1.0–1.1 with shaking at 200 rev./min, transferred to 21 °C, and induced with IPTG (isopropyl β-D-thiogalactoside; 1 mM) for 20 h. Cells were harvested by centrifugation at 5000 ***g*** and the pellets were frozen at − 80 °C. Cell pellets were thawed and extracted at room temperature (22–25 °C) with 300 ml of Bugbuster® (Novagen, Merck Biosciences, Beeston, Nottingham, U.K.) supplied in 50 mM Tris/HCl buffer [50 mM Tris (final concentration) adjusted to pH 8.0 with HCl] containing 125 μl (3125 units) of benzonase. Homogenates were then transferred to Oakridge (30 ml) centrifuge tubes, vortex-mixed for 1 min and mixed gently by inversion for 30 min. All the following procedures were then carried out at 4 °C. Homogenates were centrifuged at 28000 ***g*** for 15 min and the supernatants were decanted on ice and loaded at 5 ml/min on to a 5 ml Hi-Trap IMAC (immobilized metal-ion affinity chromatography) column (Amersham Biosciences, GE Healthcare, Chalfont St. Giles, Bucks., U.K.) charged with cobalt chloride connected to an AKTA FPLC system (Amersham Biosciences). Unbound protein was eluted at 5 ml/min with approx. 250 ml of 50 mM KH_2PO_4/K_2HPO_4 (potassium phosphate) buffer (pH 7.6) containing 0.9 M NaCl, 50 mM glycine, 5 % (v/v) glycerol and 1.56 mM Emulphogene (polyoxyethylene 10 tridecyl ether) (herein referred to as detergent buffer). Excess detergent was then removed from the bound protein by washing with 125 ml of detergent buffer without Emulphogene (buffer B), followed by 125 ml of 50 mM potassium phosphate buffer (pH 7.6) containing 0.15 M NaCl (buffer C). CYP74C3 was eluted at 5 ml/min with a linear gradient (50 ml, 10 min) from 0 to 40 mM histidine in buffer C. For purification of CYP74C3 in detergent buffer, excess detergent was not removed with buffer B and the protein was eluted with a linear gradient from 0 to 40 mM histidine in detergent buffer. In either case, fractions eluting at > 36 mM histidine were pooled and concentrated to approx. 2 ml using Amicon Ultra 10 kDa molecular-mass cut-off centrifugal filter devices (Millipore, Watford, Herts., U.K.). For detergent-free protein, the concentrate (2 ml) was then injected at 0.2 ml/min on to a Hi-load Superdex 75 26/60 gel-filtration column (Amersham Biosciences) equilibrated with 100 mM NaH_2PO_4/100 mM Na_2HPO_4 (sodium phosphate) buffer (pH 6.5) and eluted with the same buffer at 2 ml/min. For protein in detergent buffer, the concentrate (0.5 ml) was injected at 0.1 ml/min on to a Superdex 200 16/60 gel-filtration column (Amersham Biosciences) equilibrated in detergent buffer and eluted with detergent buffer at 1 ml/min. Fractions with the highest RZ (Reinheitszahl or purity index; A_{391}/A_{280}) were pooled and concentrated to 10 mg/ml.

The RZ of the final preparation (detergent-free) was 1.3, very similar to the enzyme eluted in detergent buffer. Detergent-free enzyme was snap frozen in 100 μl aliquots in liquid nitrogen and stored indefinitely at − 80 °C; enzyme in detergent buffer was best stabilized in the short term (1 month maximum) in 50 % glycerol at − 20 °C.

Untagged CYP74C3

Detergent-free untagged CYP74C3 was purified by hydrophobic interaction chromatography and gel filtration. Cell pellets from cultures were induced and extracted exactly as described for His-tagged CYP74C3, except that the crude supernatant was diluted with an equal volume of 100 mM potassium phosphate buffer (pH 7.6) containing 2 M ammonium sulphate and loaded at 5 ml/min on to a 5 ml Hi-Trap phenyl Sepharose FF (low sub) column (Amersham Biosciences) equilibrated with 50 mM potassium phosphate buffer (pH 7.6) containing 1 M ammonium sulphate. Unbound protein was eluted (as judged by A_{280}) and CYP74C3 was eluted at 5 ml/min with a linear gradient (50 ml, 10 min) from 1 to 0 M ammonium sulphate. Brown fractions (5 ml) with the highest RZ were pooled and concentrated to approx. 2 ml using Amicon Ultra 10 kDa molecular-mass cut-off centrifugal filter devices (Millipore). The concentrate was injected at 0.2 ml/min on to a Hi-load Superdex 75 26/60 gel-filtration column equilibrated with 100 mM sodium phosphate buffer (pH 6.5) and eluted with the same buffer at 2 ml/min.

Substrates and other chemicals

13-HPODE [13(S)-hydroperoxyoctadeca-(9*Z*,11*E*)-dienoic acid], 13-HPOTE (13-*S*-hydroperoxyoctadeca-9*Z*,11*E*,15*Z*-trienoic acid), 9-HPODE (9-*S*-hydroperoxyoctadeca-10*E*,12*Z*-dienoic acid) and 9-HPOTE (9-*S*-hydroperoxyoctadeca-10*E*,12*Z*,15*Z*-trienoic acid) were obtained from Larodan (Malmö, Sweden) or from Professor Mats Hamberg (Karolinska Institute, Stockholm, Sweden). They were stored in sealed vials at a concentration of 5–20 mM in ethanol under argon at − 80 °C. The exact concentration of substrate was determined using a molar absorption coefficient (ε) at 234 nm of 25 000 $M^{-1} \cdot cm^{-1}$ [36]. Emulphogene, imidazole, BI (benzimidazole), KCN (potassium cyanide), KCNS (potassium thiocyanate), pyridine, DMPhP (dimethylphenylphosphine), thiazole and azide (sodium salt) were purchased from Sigma–Aldrich (Poole, Dorset, U.K.). CO (carbon monoxide) and O_2 were supplied by BOC Gases (Manchester, U.K.). Oligonucleotides were obtained from Invitrogen or Sigma-GenoSys (Haverhill, Cambs., U.K.)

UV–visible spectroscopy

Spectra and steady-state kinetic analyses were performed using a dual-beam scanning Shimadzu UV–visible spectrophotometer (Model UV-1601; Shimadzu, Milton Keynes, U.K.). UV–visible stopped-flow spectrophotometric experiments were performed using a Hi-Tech SF-61 DX-2 double mixing apparatus (Hi-Tech Scientific, Salisbury, Wilts., U.K.) interfaced with a CU-61 control unit installed in an anaerobic glovebox operating under 1 atm (1 atm = 101.325 kPa) of N_2 containing 1 p.p.m. O_2. Stopped-flow UV–visible data were analysed with the KineticAsyst 3.0 software package (Hi-Tech Scientific). Ligand-binding studies were carried out with both the native oxidized and the dithionite ion reduced forms of CYP74C3.

EPR spectroscopy

EPR spectroscopy was performed on a Bruker ELEXYS 500 spectrometer with an ER049X SuperX microwave bridge and an shq cavity (Bruker Analytische Messtechnik). Low-temperature experiments were performed using an Oxford Instruments ESR-900 cryostat and ITC3 temperature controller. EPR spectra were simulated using the computer program SimFonia (Bruker). EPR spin concentration measurements were made by double integration and comparison with a copper EDTA standard under non-saturating conditions. EPR spectra were measured at 10 K and 2 mW microwave power [37].

Haem incorporation

Haem content and type were determined from quantification of the pyridine haemochrome using alkali-denatured protein and a molar absorption coefficient for the reduced–oxidized difference spectrum of 28 360 $M^{-1} \cdot cm^{-1}$ at 556.4 nm [38].

Standard activity assay

The standard assay mixture (0.5 ml) contained 20 μM substrate in 100 mM sodium phosphate buffer (pH 6.5). The decrease in A_{234} was followed for 20–60 s at 25 °C and converted into moles of substrate using a molar absorption coefficient of 25 000 $M^{-1} \cdot cm^{-1}$ [36]. The initial linear region of the progress curves was used to calculate rates. CYP74C3 concentration was determined from the haem content using a calculated molar absorption coefficient at 391 nm of 120 000 $\pm$ 24 000 $M^{-1} \cdot cm^{-1}$. Protein content was estimated using the Bradford assay [39] or BCA (bicinchoninic acid) assay (Pierce, Perbio Science, Cramlington, Northumberland, U.K.) according to the manufacturer's instructions, with BSA as a standard.

Kinetic properties

Steady-state kinetic data were collected using Shimadzu kinetics software (version 2.7). K_m and k_{cat} for substrates and K_d for Emulphogene, cyanide, imidazole and DMPhP were calculated by fitting the datasets to a one-site saturation model for simple ligand binding using SigmaPlot 8 (Sigma–Aldrich). The difference in the amplitude of absorbance at the Soret band of the native and liganded enzyme was plotted as a function of ligand concentration; enzyme and ligand were incubated for at least 5 min before spectra were recorded. All K_d measurements were carried out in 100 mM sodium phosphate buffer at pH 6.5, or, for KCN solutions, adjusted to pH 9.5, 9.0 or 8.0 with KOH or HCl. Substrate specificity was determined by comparing k_{cat}/K_m. Predicted micelle concentration (μM) was calculated using the equation:

$$[\text{Micelle}] = ([\text{total detergent}] - \text{c.m.c.})/N$$

where aggregation number N = number of monomers/micelle (88 for Emulphogene [40]) and c.m.c. is critical micellar concentration. The 'positive' data were used to estimate the K_d for binding of an Emulphogene micelle.

GC–MS analysis

The spectrophotometric assay used to measure CYP74C3 activity monitored only substrate disappearance and was unable to distinguish between HPL and AOS activities. Non-volatile products were extracted from reaction mixtures essentially as described in [41]. A reaction mixture (10 ml) containing 13-HPOTE (40 μM) and either CYP74C3 in detergent buffer (20 μg) or detergent-free CYP74C3 (2 μg) in 100 mM sodium phosphate buffer (pH 6.5) was incubated at 22 °C for 15 min, adjusted to pH 4.3 with dilute acetic acid and applied to a conditioned Sep-Pak C18 cartridge (Waters, Elstree, Herts., U.K.). Air was then forced through the cartridge to remove water and bound products were eluted with

methanol. Reduction, methylation and trimethylsilylation for GC-MS analysis were carried out exactly as described in [41].

Protein sequencing and SDS/PAGE analysis

The amino acid sequence of CYP74C3 predicted from the cDNA sequence was confirmed by a combination of MALDI–TOF (matrix-assisted laser-desorption ionization–time-of-flight) MS, Edman sequencing and ISD (in source decay) (E. J. Belfield, R. K. Hughes, I. Galetich, K. Wilson, M. Naldrett and R. Casey, unpublished work). SDS/PAGE was carried out using NuPAGE (4–12 %, w/v, gradient Bis-Tris gels) with Mes SDS running buffer (50 mM Mes and 50 mM Tris buffer, pH 7.3, containing 3.5 mM SDS and 1 mM EDTA) and SeeBlue Plus 2 protein markers according to the manufacturer's instructions (Invitrogen).

Gel filtration

The molecular mass (M; relative to protein standards) of native CYP74C3 in detergent-free buffer was determined by gel filtration on a Superdex 75 26/60 column. The molecular mass (M) of the unknown was determined from a plot of log M (y) versus V_e/V_o (x) and the data were fitted by linear regression (correlation coefficient 0.996) to the equation:

$$y = -1.2496x + 6.4101$$

The molecular mass of native CYP74C3 in detergent buffer was determined on a Superdex 200 16/60 column. The data were fitted by linear regression (correlation coefficient 0.988) to the equation:

$$y = -1.5385x + 7.4166$$

Gel filtration of CYP74C3 in 100 mM sodium phosphate buffer (pH 6.5) containing Emulphogene at 0.08 mM, slightly below the c.m.c. of 0.125 mM [40], was also carried out using a calibrated Superdex 200 HR 10/300 column (Amersham Biosciences) eluted at 0.5 ml/min.

Analytical ultracentrifugation

Sedimentation velocity and equilibrium experiments were carried out to determine the effects of protein concentration, ionic strength, pH and detergent buffer on the oligomeric state of CYP74C3.

Sedimentation velocity analysis of detergent-free CYP74C3 (0.5 and 1.0 mg/ml in 100 mM sodium phosphate buffer, pH 6.5) was carried out in an Optima XL-A ultracentrifuge (Beckman Coulter, High Wycombe, Bucks., U.K.) at 50 000 rev./min and 20.0 °C (An-60 Ti rotor), with solute distributions recorded using UV-absorption optics at 280 nm with scans every 3.5 min. Experiments were repeated using CYP74C3 at the same protein concentrations and also from 5 to 15 mg/ml using the interference optical system in an XL-I ultracentrifuge (Beckman Coulter). Similar experiments on CYP74C3 (1 mg/ml) were carried out as above after buffer exchange into 10, 50 or 100 mM sodium phosphate buffer (pH 6.5) and into 100 mM sodium phosphate buffer at pH 5.8, 6.9 and 7.8. To study the effects of detergent buffer on CYP74C3 oligomerization, sedimentation velocity experiments were carried out as above with CYP74C3 (0.5 and 1 mg/ml) in detergent buffer. Scans were recorded at 232 nm every 3.5 min. The raw sedimentation data were analysed using the procedure SEDFIT (a software program for the analysis of analytical ultracentrifugation and other hydrodynamic data) [42]. Both the $c(s)$ and least square $g(s)$ models were employed for the analysis of the sedimentation data and for the determination of the apparent sedimentation coefficient. Because of the very heterogeneous nature of CYP74C3 in association with detergent, an overlay of the $c(s)$ model on the least square $g(s)$ distribution was used to identify the peaks in the least square $g(s)$ plot. In addition, multiple Gaussians were fitted to the least square $g(s)$ profile obtained from SEDFIT using the ROBUST fitting algorithm within the software program PRO-FIT (QuantumSoft, Uetikon am See, Switzerland) to allow an approximation of the proportion of the oligomers present in solution.

The Optima XL-A ultracentrifuge (Beckman Coulter) was also used to determine the weight-average molecular mass, M_w, of detergent-free CYP74C3 using low-speed sedimentation equilibrium. Samples (0.5 or 1 mg/ml detergent-free CYP74C3 in 100 mM sodium phosphate buffer, pH 6.5) were centrifuged at 20 000 rev./min and 20.0 °C (An-60 Ti rotor) and scans were taken at 280 nm every 2 h until equilibrium was reached (after 24 h). To obtain the M_w of CYP74C3 in detergent buffer, data were analysed using the MSTARA algorithm [43]. The effects of thermodynamic non-ideality were assumed to be negligible.

Other parametric calculations

The partial specific volume ($\bar{v}$) of detergent-free CYP74C3 in 100 mM sodium phosphate buffer (pH 6.5) was calculated from the predicted amino acid composition using the routine SEDNTERP [44] to be 0.744 ml/g. The partial specific volume of CYP74C3 in detergent buffer was measured by determination of the relative viscosity and density using a viscometer and an Anton-Paar density meter respectively as this included a contribution from micellar association of the protein. The average molecular mass of an Emulphogene micelle has been reported to be 56.0 kDa [40]. We also made our own approximation by applying the empirical equations of Squire and Himmel [45] in the software BIOMOLS (http://www.nottingham.ac.uk/ncmh/unit/method.html#Software). On the assumption that micelles are globular particles with a sedimentation coefficient close to 1 S and using the calculated value for $\bar{v}$ of 0.945 ml/g, the molecular mass of an Emulphogene micelle was approx. 68 kDa. An average value of approx. 62 kDa was used for further calculations.

Gel-filtration analysis of micelle formation

An aqueous solution of 13-HPOTE in 100 mM sodium phosphate buffer, pH 6.5 (80 mM, 30 μl), with and without an equimolar amount of Emulphogene (80 mM), was injected on to a Sephadex G-50 (Amersham Biosciences) column (27 cm × 0.275 cm, 1.6 ml) in 100 mM sodium phosphate buffer (pH 6.5) and eluted at 0.1 ml/min. Standards (30 μl) of known molecular mass were: Emulphogene detergent micelle (62 kDa, 80 mM), detergent-free CYP74C3 monomer (56.8 kDa, 20 μM); carbonic anhydrase (29 kDa, 3 mg/ml); vitamin B_{12} (1.355 kDa, 0.1 mg/ml), Blue Dextran (2000 kDa, 2 mg/ml) and N-2,4-dinitrophenyl-DL-methionine sulphoxide (331.3 Da, 0.1 mg/ml).

RESULTS

DNA sequence analysis of the clones pDEST14HPL-F + 8 and pDEST14HPL-F-8 revealed that the predicted amino acid sequence of the protein expressed from both constructs was identical with that of the original cDNA clones. MALDI–TOF MS, Edman sequencing and ISD were used to confirm unambiguously that the sequence of the entire protein expressed from pDEST17HPL-F + 7 was identical with that predicted from the original cDNA clone, except for the replacement of methionine as the start codon with an asparagine residue (E. J. Belfield, R. K. Hughes,

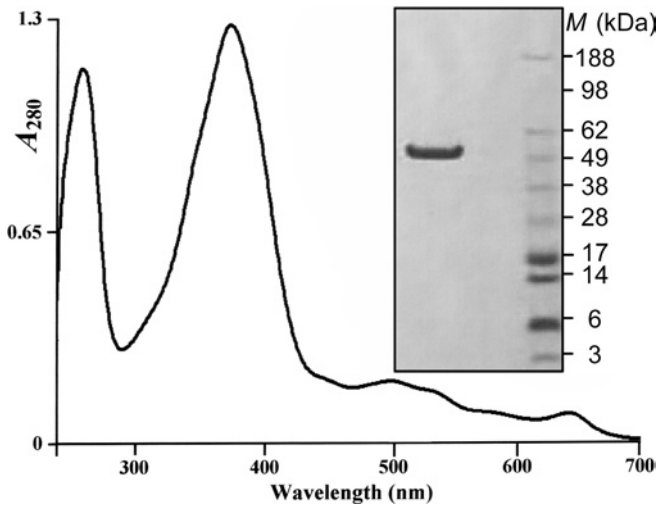

Figure 1 UV–visible spectrum and SDS/PAGE analysis of purified detergent-free CYP74C3

Spectrum of detergent-free CYP74C3 (10.5 μM) in 100 mM sodium phosphate buffer (pH 6.5) and SDS/PAGE analysis of the same preparation (52.5 pmol) (inset). Abbreviation: *M*, molecular mass.

Table 1 Kinetic parameters and substrate specificity of purified CYP74C3 before and after removal of detergent and after re-activation with detergent

Values shown are the means ± S.E.M. for at least six determinations on two different enzyme preparations.

Kinetic parameter	+ Detergent	Detergent-free	Re-activated*
k_{cat} (s^{-1})†			
13-HPOTE	514 ± 11	68 ± 5	657 ± 14
13-HPODE	361 ± 19	59 ± 3	493 ± 17
9-HPOTE	24 ± 2	8 ± 0.4	30 ± 1
9-HPODE	197 ± 6	44 ± 2	185 ± 7
K_m (μM)			
13-HPOTE	3.3 ± 0.4	20.9 ± 1.7	4.4 ± 0.6
13-HPODE	10.3 ± 2.1	102.0 ± 11.8	14.7 ± 1.9
9-HPOTE	39.1 ± 7.2	81.6 ± 9.7	51.7 ± 4.4‡
9-HPODE	15.3 ± 1.4	84.5 ± 10.1	25.8 ± 2.2‡
k_{cat}/K_m ($\mu M^{-1} \cdot s^{-1}$)			
13-HPOTE	155.8	3.2	149.3
13-HPODE	35.0	0.6	33.5
9-HPOTE	0.6	0.1	0.6
9-HPODE	12.9	0.5	7.2
Substrate specificity (% 13-HPOTE)			
13-HPOTE	100	100	100
13-HPODE	23	19	22
9-HPOTE	0.4	3	0.4
9-HPODE	8	16	5

* With 5 mM Emulphogene.

† Assuming one active site per monomer of molecular mass 56.8 kDa.

‡ All data were fitted for substrate concentrations up to 160 μM, except for these two values where tighter fits were achieved using the data for concentrations up to 80 μM.

I. Galetich, K. Wilson, M. Naldrett and R. Casey, unpublished work).

Extraction of soluble His-tagged CYP74C3 activity and binding of this activity to an IMAC column required the presence of detergent, suggesting that CYP74C3 is associated with membranes in *E. coli*. This localization was confirmed in ultracentrifugation studies under detergent-free conditions where activity was almost exclusively associated with a detergent-solubilized membrane-enriched fraction (results not shown). The purified detergent-free CYP74C3 preparation was homogeneous as judged by SDS/PAGE (Figure 1). Optimization of the purification using Co- instead of Ni-IMAC was essential to remove minor contamination by an *E. coli* peptidylprolyl *cis–trans* isomerase [46] that was clearly identified by MALDI–TOF analysis (results not shown). This protein had a subunit molecular mass of 22 kDa (44 kDa dimer in solution) but ran anomalously in SDS/PAGE with an apparent subunit molecular mass of approx. 30 kDa. Elution with histidine rather than imidazole was essential to produce an active enzyme with the characteristic UV–visible spectrum shown in Figure 1; the spectrum was not dependent on protein concentration. The protein had a Soret band at 391 nm, and major features at 508, 545 and 644 nm. Elution of the enzyme with imidazole produced a virtually inactive enzyme (results not shown). Analysis using the pyridine haemochrome method confirmed that the enzyme had a full complement of type b haem (0.93 ± 0.16 mol/mol protein). The RZ of pure protein was 1.3. The molar absorption coefficient at 391 nm was calculated to be 102 000 and 141 000 $M^{-1} \cdot cm^{-1}$ using the Bradford assay and BCA assay respectively. The mean value of 120 000 ± 24 000 $M^{-1} \cdot cm^{-1}$ was used to calculate CYP74C3 concentration. The UV–visible spectrum shown in Figure 1 was of the protein purified as a monomer (see later). In some circumstances after gel filtration, however, a small proportion of soluble aggregated protein was also observed, which eluted at the void volume and had the same purity (as judged by SDS/PAGE) but a lower RZ (~1.1). The latter was presumably due to the higher absorbance of the aggregates at 280 nm relative to haem. The UV–visible spectrum of CYP74C3 purified without removing the Emulphogene detergent had a very similar spectrum and purity to the detergent-free protein, as judged by SDS/PAGE, but the same RZ as the detergent-free enzyme (1.3) (results not shown). The purity of untagged CYP74C3 expressed from pDEST14HPL-F + 8 was estimated by SDS/PAGE to be approx. 80–85 %.

GC-MS analysis confirmed that detergent-free CYP74C3 was an HPL and not an AOS since 12-oxo-(9*Z*)-dodecenoic acid was the major non-volatile product from a reaction with 13-HPOTE as substrate (results not shown): *m/z* (ion attribution; relative intensity), 300 (M^+; 0.06 %), 285 ($M^+ - CH_3$; 3.2 %), 253 ($M^+ - CH_3O_2$; 11.6 %), 103 (CH_2OTMS+; 100 %; where TMS is trimethylsilyl), 73 (TMS+; 91.4 %) [41]. The isomerization product, 12-oxo-(10*E*)-dodecenoic acid (traumatin), was also detected: *m/z* (ion attribution; relative intensity), 300 (M^+; 1.6 %), 285 ($M^+ - CH_3$; 8.7 %), 253 ($M^+ - CH_3O_2$; 51.9 %), 129 (C_3H_4OTMS+; 100 %) and 73 (TMS+; 81.1 %) [41].

Detergent-free CYP74C3 exhibited a broad pH profile with activity maxima between pH 5.5 and 7.5 with all four substrates tested. Activity was still significant outside this range for 13-hydroperoxides, but significantly decreased above pH 8.0 for 9-hydroperoxides (results not shown). pH 6.5 was selected as the optimum pH for standard assays. A comparison of the catalytic efficiencies (k_{cat}/K_m) of CYP74C3 with the four substrates (Table 1) confirms that the preferred substrate by far was 13-HPOTE, and the efficiency of turnover of 13-HPODE, 9-HPOTE and 9-HPODE was only 23, 0.4 and 8 % respectively of that with 13-HPOTE. With 13-HPOTE as the substrate, the k_{cat} of CYP74C3 in detergent buffer was approx. 8-fold higher than detergent-free enzyme (Table 1) and was associated with a 6-fold decrease in affinity for this substrate. The effects of detergent removal on the activity of CYP74C3 with the other three substrates were similar. Detergent removal reduced the catalytic efficiency of CYP74C3 to a level that was only 2 % (13-HPOTE

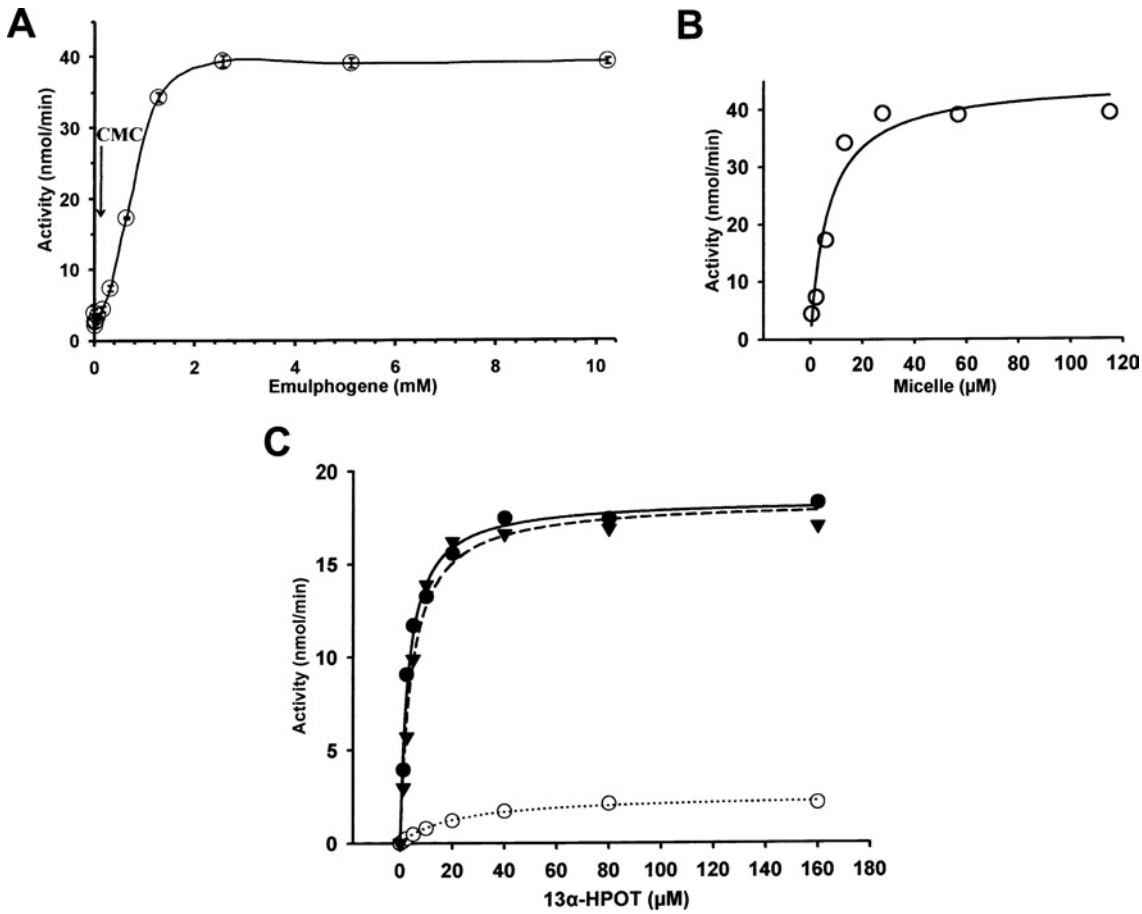

Figure 2 Re-activation of detergent-free CYP74C3 with detergent

(**A**) Dose–response curve for re-activation of detergent-free CYP74C3 with the detergent Emulphogene. Detergent-free CYP74C3 was incubated with an equal volume of 100 mM sodium phosphate buffer (pH 6.5) or containing detergent (0.01–10.24 mM Emulphogene) for 15 min on ice. Samples (1.2 pmol) were then assayed for HPL activity in the standard assay with 20 μM 13-HPOTE. The c.m.c. of Emulphogene at 0.125 mM is shown. Results shown are the means $\pm$ S.E.M. for at least six determinations on two different enzyme preparations. (**B**) Plot of predicted micelle concentration versus activity for calculation of K_d for Emulphogene binding. (**C**) Fit of velocity–substrate curves to one-site saturation model in SigmaPlot for detergent-free CYP74C3 (1.0 pmol; ○···○), CYP74C3 purified in detergent buffer (0.5 pmol; ●-●) and detergent-free CYP74C3 after re-activation with 5 mM Emulphogene (0.5 pmol; ▼-▼).

and 13-HPODE), 17 % (9-HPOTE) and 4 % (9-HPODE) of that observed when the enzyme was purified without detergent removal; there was no major effect of detergent removal on substrate specificity.

Detergent-free CYP74C3 could be re-activated with the detergent Emulphogene at a concentration exceeding 2.6 mM (Figure 2A). No re-activation was observed with Emulphogene at a concentration of 0.1 mM, which was slightly below the c.m.c. The K_d for the binding of Emulphogene micelles to CYP74C3 was estimated as 6.9 ± 1.1 μM (Figure 2B). The k_{cat}, K_m and k_{cat}/K_m values for re-activated CYP74C3 with all four substrates were very similar to those recorded for CYP74C3 purified without detergent removal (Table 1), so, as observed for detergent removal, re-activation with detergent also had no effect on substrate specificity. Re-activation of detergent-free CYP74C3 was observed with concentrations of 13-HPOTE (and the other three substrates; results not shown) up to 160 μM (Figure 2C); at concentrations > 240 μM, there was substantial substrate inhibition (results not shown). These substrates may, however, start to form micelles at concentrations well above this concentration, though no c.m.c., or behaviour to form micelles, has been reported. Sephadex G-50 chromatography indicated that aqueous solutions of 13-HPOTE at concentrations up to 80 mM, vitamin B_{12} and 2,4-dinitrophenyl-DL-methionine sulphoxide were all retained to some degree by a Sephadex G-50 column and eluted at 2.16–2.32 ml; in contrast, Blue Dextran, carbonic anhydrase, detergent-free CYP74C3 monomer and Emulphogene micelle were all excluded from the matrix and eluted at 1.00–1.09 ml. A sample containing equimolar amounts (5 mM) of 13-HPOTE and Emulphogene separated as two overlapping peaks with elution volumes of 1.12 and 2.09 ml, very similar to that of the Emulphogene micelle and 13-HPOTE monomer respectively (results not shown). These results showed that 13-HPOTE did not form any micelles, or mixed micelles with Emulphogene.

The effects of ligand binding or reduction by sodium dithionite on the UV–visible spectrum and the spin state of the haem iron on detergent-free CYP74C3 are summarized in Supplementary Table 2 (http://www.BiochemJ.org/bj/395/bj3950641add.htm). For selected ligands, the UV–visible spectra are shown in Figure 3. A shift in the UV–visible spectrum to 452 nm was observed after binding CO to the dithionite-reduced enzyme (inset to Figure 3), which is typical of cytochrome P450-like enzymes. The dithionite-reduced enzyme exhibited a shift in the Soret band from 390 to 408 nm, consistent with high-spin Fe(II). The UV–visible spectra of CYP74C3 with imidazole or cyanide bound were typical of a low-spin haem iron with red shifts for both Soret

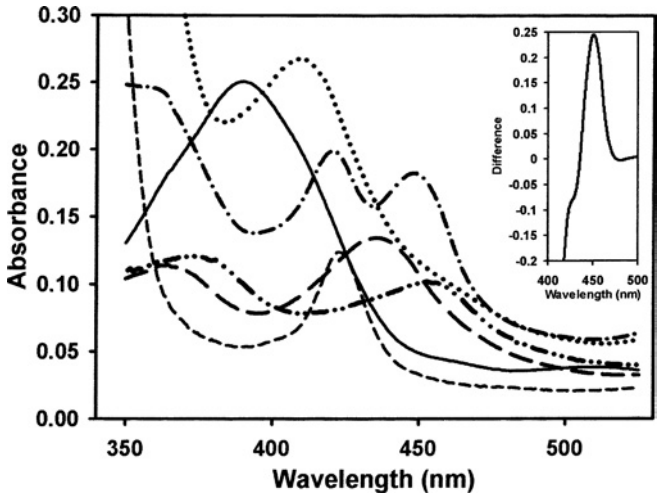

Figure 3 Ligand-binding studies of detergent-free CYP74C3

UV–visible spectra of ligand-bound forms of oxidized native CYP74C3 (2 μM; ——); KCN (100 mM; — — —); imidazole (50 mM; - - - -); DMPhP (250 mM; — ●● —). The spectra of dithionite (50 mM) reduced CYP74C3 (2 μM) before (●●●●●) and after (— ● —) reaction with CO (~1 mM) are also shown; inset, the difference spectrum for CO binding. The increase in absorbance below 400 nm is due to the large excess of sodium dithionite used. All spectra were recorded at pH 6.5 in 100 mM sodium phosphate buffer (pH 6.5) at 25 °C, 1 cm path length.

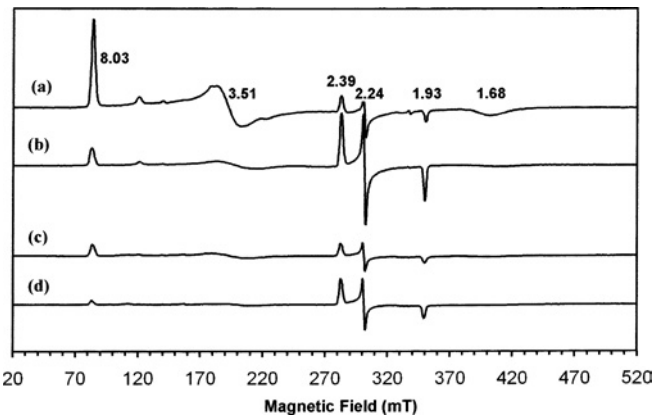

Figure 4 Effects of 13-HPOTE or detergent on the EPR spectrum of detergent-free CYP74C3

EPR spectra shown are: (**a**) 240 μM resting enzyme and (**b**) after reaction with 5 mM Emulphogene or (**c**) 2.4 mM 13-HPOTE. The sample in (**b**) was thawed and reacted with 2.4 mM 13-HPOTE prior to immediate refreezing in liquid nitrogen and the EPR spectrum (**d**) was recorded again. The *g* values of the peaks corresponding to high- and low-spin haem iron are shown.

and visible bands. The imidazole complex exhibited bands at 366, 426, 544 and 547 nm (Figure 3) with a K_d at pH 6.5 of 362.5 ± 120.4 mM. Measurements by stopped-flow absorption showed that the kinetics of imidazole binding was biphasic (results not shown). The cyanide complex exhibited bands at 365, 434, 539 and 566 nm and K_d values of 105.1 ± 24.0 and 1507.9 ± 448.4 mM respectively were obtained at pH 9.0 and 8.0. The time course for cyanide binding monitored at 440 nm using the stopped-flow diode-array data was also biphasic (results not shown). Ferrous low-spin haem iron spectrophotometric signatures were also observed for O_2, pyridine and BI with red-shifted Soret and visible bands (see Supplementary Table 2 at http://www.BiochemJ.org/bj/395/bj3950641add.htm). Binding of the sulphur- and phosphorous-containing ligands thiazole and DMPhP gave low-spin haem iron bands with large Soret band shifts (see Supplementary Table 2 at http://www.BiochemJ.org/bj/395/bj3950641add.htm); the DMPhP complex has bands at 375, 453 and 563 nm (Figure 3) with a K_d at pH 6.5 of 5.3 ± 0.8 mM. Thiocyanate and azide binding resulted in a mixture of high and low-spin haem iron bands (see Supplementary Table 2 at http://www.BiochemJ.org/bj/395/bj3950641add.htm).

EPR spectroscopy indicated that the spectrum of the resting enzyme contained a mixture of high- and low-spin haem iron with *g* factors of 8.03, 3.51, 1.68, and 2.39, 2.24, 1.93 respectively (values from simulation of spectra), in the ratio of 2.5:1 (Figure 4a). Addition of Emulphogene at a concentration of 2.4 mM, well above the c.m.c., to resting enzyme (240 μM), resulted in a change in the ratio of high to low spin haem iron to 1:5.5, but with no change in the total EPR concentration (Figure 4b). The addition of 13-HPOTE at 2.4 mM to resting enzyme (240 μM) resulted in a 60 % loss of EPR intensity and a ratio of high to low spin haem iron of 1:2 (Figure 4c). Subsequent addition of 13-HPOTE at 2.4 mM to the enzyme sample previously reactivated with 2.4 mM Emulphogene resulted in a 50 % reduction in the total concentration of the EPR signal and a ratio of high to low spin haem iron signal of 1:6 (Figure 4d). The UV–visible spectra and specific activities of the resting and detergent-reactivated enzymes after EPR were indistinguishable from those before the analysis (results not shown). Similar effects were also seen with resting enzyme at 24 μM, which suggests that there was no concentration dependency. At a concentration of 0.1 mM, slightly below the c.m.c. of Emulphogene, both Emulphogene and 13-HPOTE had no effect on the EPR spectrum of resting enzyme at 24 μM (results not shown). Changes in the spin state of the haem iron, induced by detergent micelles, were also associated with subtle changes in the UV–visible spectrum (results not shown). Addition of 1.56 mM Emulphogene to the detergent-free enzyme at 10.2 μM resulted in a change in the Soret region; the peak at 391 nm was shifted to 393 nm and a shoulder developed at 420 nm with an isosbestic point at 401 nm. Similar changes at longer wavelengths were observed; the features at 508 and 644 nm were reduced, the feature at 545 nm increased slightly and a new feature appeared at 568 nm with isosbestic points at 454, 530, 581 and 669 nm (results not shown). No clear changes in the UV–visible spectrum were observed during the reaction of 10.2 μM CYP74C3 in the presence and absence of 5 mM Emulphogene, with 100 μM or 2.4 mM 13-HPOTE, nor with detergent-free 10.2 μM CYP74C3 and 0.08 mM Emulphogene (results not shown).

Oligomeric state of detergent-free CYP74C3

The molecular mass of His-tagged CYP74C3, based on the protein sequence and predicted from the cDNA, was 56.8 kDa. This was consistent with the value determined for the native protein by gel filtration (relative to globular protein standards) of 55.2 kDa (Figure 5). These measurements, and dynamic light scattering (results not shown), indicated that detergent-free CYP74C3 was a monomer. No dimer, which, if present, would have been cleanly separated from monomer, could be detected by gel filtration (Figure 5), and activity could be detected only in the monomer fraction. Under the conditions in the ultracentrifuge, analysis of the sedimentation velocity data indicated that detergent-free CYP74C3 at 1 mg/ml was also almost exclusively a monomer with a sedimentation coefficient of 3.5 S (inset to Figure 5). A corresponding weight-average molecular mass, M_w, of

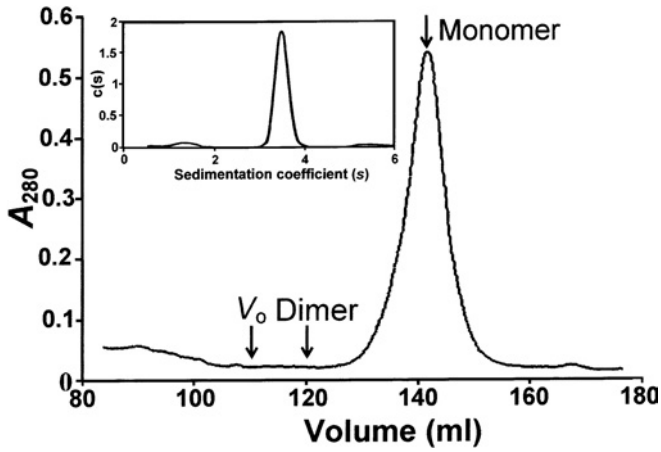

Figure 5 Gel-filtration analysis of purified detergent-free CYP74C3

Purified CYP74C3 (2 ml, 5.6 mg) was loaded on to a Superdex 75 26/60 column equilibrated and eluted at 1 ml/min with 100 mM sodium phosphate buffer (pH 6.5). Peak positions for species with molecular mass corresponding to the size of a protein monomer and dimer are shown. Inset: sedimentation velocity analysis of detergent-free CYP74C3; apparent sedimentation coefficient distribution of detergent-free CYP74C3 evaluated at 1 mg/ml by the *c*(*s*) analysis module in SEDFIT using sedimentation velocity data. Refer to the Experimental section for details.

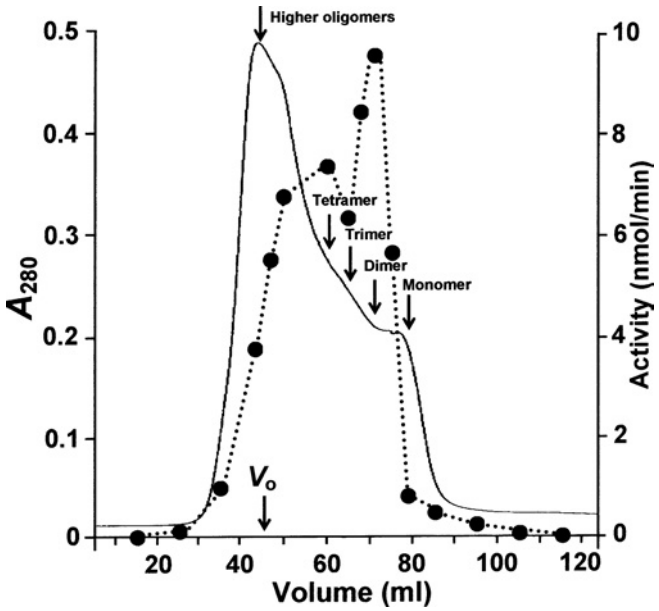

Figure 6 Gel-filtration analysis of purified CYP74C3 in detergent buffer

Purified CYP74C3 (0.5 ml, 5 mg) in detergent buffer was loaded on to a Superdex 200 16/60 column equilibrated and eluted in detergent buffer at 0.5 ml/min. Fractions were monitored at A_{280} (——) and for CYP74C3 activity (·····). Peak positions for species with molecular mass corresponding to the size of different oligomers are shown. The closed circles denote the elution volumes at which the activities of CYP74C3 were determined.

55 ± 2 kDa was determined from sedimentation equilibrium studies on CYP74C3 at 1 mg/ml, in excellent agreement with the gel-filtration result. At higher protein concentrations (up to 15 mg/ml), a small amount of aggregated protein (5–11 S) was detected by sedimentation velocity. In addition, there was some evidence for the presence of dimers, but these were not in reversible equilibrium with the monomers (increase in loading concentration caused no increase in dimers relative to monomers). CYP74C3 at 15 mg/ml was therefore almost exclusively monomeric with an average sedimentation coefficient of 3.7 S. As the ionic strength was decreased from 100 to 10 mM, the proportion of monomer in the sample decreased and the proportion of aggregated protein (5–11 *s*) generally increased. The proportion of monomer also increased with an increase in pH from 5.8 to 7.9. Again, some aggregated protein (5–10 *s*) was present along with the monomer.

We carried out a gel-filtration analysis of untagged CYP74C3, which confirmed the presence of active monomers, plus a small amount of soluble aggregated protein that eluted at the void volume (results not shown), exactly as observed for the tagged protein. This suggested that the His tag plus Gateway® *att* recombination sequence had no effect on the oligomeric state. Similarly, CYP74C3 expressed without the first 11 amino acids at the N-terminus (MASSSETSSTN) was also almost exclusively monomeric (results not shown), suggesting that the N-terminal extension sequence of CYP74C3 was not involved in determining oligomeric state.

Oligomeric state of CYP74C3 in detergent buffer

Gel-filtration analysis of CYP74C3 in detergent buffer indicated that it formed only a small amount of monomer, as judged from the peak position on a calibrated Superdex 200 16/60 column (Figure 6). The smallest active oligomer eluted at a position corresponding to the size of a protein dimer, with most of the protein forming a heterogeneous mixture of non-resolved higher oligomers. In order to attempt to resolve the sizes of the individual components in the mixture, the sample was analysed by analytical ultracentrifugation, which confirmed the gel-filtration analysis and indicated that CYP74C3 formed a broad range of oligomers. The peaks identified in the *g*(*s*) distribution using the sedimentation velocity data for CYP74C3 at 0.5 mg/ml indicated that there were several oligomers present with apparent sedimentation coefficients of 3.2, 5.3, 7.0, 9.4, 12.1, 14.8 and 17 S (see Supplementary Figure 7 at http://www.BiochemJ.org/bj/395/bj3950641add.htm). It is plausible that the formation of micelle–protein complexes would allow sedimentation to occur more slowly than the pure protein because of the high partial specific volume of the detergent. We may note that on the basis of the 3.2 *s* species being monomeric, then on the basis of the frictional ratio being constant over all species, a 'ladder' of incremental *n*-mers would have predicted sedimentation coefficients of 3.2, 5.0, 6.5, 8.1, 9.4, 10.6 and 11.7 S. The rather higher values seen probably reflect a growing protein/detergent ratio in the micelles as the order of oligomerization increases. It is possible that this happens via successive monomers being added into existing micellar units. A comparison of the activities of CYP74C3 oligomers after gel filtration in a buffer containing Emulphogene at 1.56 mM, well above the c.m.c., indicated that most activity was found at a peak position corresponding to the size of a dimer (Figure 6). The trimer, tetramer, higher oligomers and monomer had 67, 51, 20 and 10 % respectively of the specific activity of the dimer (results not shown).

When CYP74C3 in detergent buffer was applied to a gel-filtration column equilibrated under detergent-free conditions, a number of higher oligomers were detected, but the smallest, most active, species eluted at a position corresponding to a molecular mass of approx. 87 kDa (results not shown). Gel-filtration analysis of CYP74C3 in 100 mM sodium phosphate buffer (pH 6.5) containing Emulphogene at 0.08 mM (slightly below the c.m.c.) confirmed that it was almost entirely monomeric as observed for the detergent-free protein (results not shown). The specific activity and kinetic parameters of detergent-free CYP74C3 expressed with and without the first 11 amino acids were indistinguishable from those for the full-length protein (results not shown).

DISCUSSION

CYP74C3 from *M. truncatula* is a cytochrome P450 enzyme with HPL activity. CYP74C3 exhibited dual specificity, turning over both 9- and 13-hydroperoxides, and in this respect it is very similar to CYP74C1 [27] and CYP74C2 [28]. The RZ of 1.3 and molar absorption coefficient at 391 nm of $120\,000 \pm 24\,000\ M^{-1} \cdot cm^{-1}$ are the first reported for any HPL. The RZ is identical with that of coral AOS [47]. The molar absorption coefficient at 391 nm is also very similar to that reported for coral AOS (at 406 nm) of $100\,000\ M^{-1} \cdot cm^{-1}$ [47] and for flax AOS (at 392 nm) of $140\,000\ M^{-1} \cdot cm^{-1}$ [48]. It is not possible to make comparisons with the RZ of other purified HPLs because the published spectra show only absorbance above 300 nm [13,21,28]; a molar absorption coefficient of $39\,000\ M^{-1} \cdot cm^{-1}$ has been calculated for CYP74B3 [21], but the purity of the enzyme preparation and haem content were not reported. UV–visible and EPR spectroscopy of oxidized CYP74C3 both indicated that the protein was typical of a thiolate-ligated penta-co-ordinate, ferric high-spin haem iron-containing enzyme, with the sixth position accessible for ligand binding (see [48]); some low-spin haem iron was also present. The *g* values recorded for the resting enzyme were very similar to those reported for CYP74B1 (purified without detergent removal) at 8.05, 3.5 and 1.65 (high-spin haem iron) and 2.38, 2.24 and 1.92 (low-spin haem iron) [24]. Features in the UV–visible spectrum of detergent-free CYP74C3 were very similar to flax AOS (Soret band at 392 nm) [48], but quite different from that of detergent-free CYP74B4 (Soret band at 420 nm) [49]; the latter was attributed to the major presence of low-spin haem iron. The Soret band at 406 nm for coral AOS [47] was, like CYP74C3, attributed to a major presence of high-spin haem iron. The positions of the α and β bands at 545 and 508 nm respectively in CYP74C3 are very different from those observed for most classical and non-classical cytochrome P450 enzymes (for example, at 569 and 535 nm in CYP2B4 [49] and at 567 and 535 nm in thromboxane synthase [5]). They are, however, more similar to those at 540 and 512 nm in flax AOS [48], and at 534 and 500 nm in coral AOS [47], both of which are CYP74 enzymes that were soluble in the absence of detergent.

Ligand-binding studies confirm that CYP74C3 is a cytochrome P450 enzyme. Previously, only dithionite reduction [13,18,21,24], CO [18,21,28] and NO [24] binding have been reported for an HPL. Imidazole, cyanide, dioxygen, thiazole, azide, pyridine, thiocyanate and BI have now all been shown to bind to CYP74C3. The resulting spin states and UV–visible spectra have been determined and compared with other CYP74 enzymes, coral AOS and selected classical cytochrome P450 enzymes (see Supplementary Table 2 at http://www.BiochemJ.org/bj/395/bj3950641add.htm). The K_d for three ligands, imidazole, cyanide and DMPhP, have been determined. The UV–visible spectra of the cyanide and imidazole complexes of CYP74C3 are very similar to CYP2B4 [50], CYP1A2 [50], CYP74B1 [24] and coral AOS [47]. Features in the DMPhP and BI complexes of CYP2B4 [50] and CYP1A2 [50], and the azide complex of coral AOS [47], are also very similar to those of CYP74C3. The kinetics for cyanide binding is pH-dependent due to the anticipated effects of the changes in ligand protonation state. The approx. 14-fold increase in K_d for cyanide (pK_a 9.1 in water [51]) at pH 8.0 compared with that at pH 9.0 strongly suggests that CN^- and not HCN is the form that binds. The K_d (362 mM) for imidazole binding to CYP74C3 is notably four orders of magnitude higher than thromboxane synthase (33 μM) [5], which has also been shown to exhibit biphasic kinetics with this ligand.

Detergent micelles increased the k_{cat} of CYP74C3 by up to an order of magnitude through improvements in substrate binding. The very tight binding of 13-HPOTE, with a K_m of only 3.3 μM, is among the highest reported for any HPL. The very high catalytic-centre activity of up to 657 s^{-1} is the first reported for an HPL and is typical of a CYP74 enzyme, although somewhat lower than 4700 or 1200 s^{-1}, which were observed for flax AOS [48] and CYP74A2 [10] respectively, but this probably reflects differences in the reaction mechanisms of HPL and AOS. The k_{cat}/K_m of up to $1.6 \times 10^8\ M^{-1} \cdot s^{-1}$ demonstrates that CYP74C3 is an extremely efficient catalyst matching that of carbonic anhydrase I [52]. This is particularly remarkable for an enzyme whose reaction mechanism involves the scission of a C–C bond in a relatively large (C_{18}) fatty acid hydroperoxide substrate. Micelle-induced changes in catalytic-centre activity were associated with subtle changes in both the Soret and visible regions of the spectrum of CYP74C3; the development of a shoulder at 420 nm and a new feature at 568 nm upon addition of detergent micelles to detergent-free CYP74C3 suggested a shift in equilibrium towards low-spin haem iron, which was confirmed by EPR spectroscopy. The UV–visible spectra of CYP74C3, CYP74B1 [24] and CYP74B3 [21], purified without detergent removal, were very similar to one another, with a major Soret band at 390–393 nm, characteristic of high-spin haem iron. The UV–visible spectrum of CYP74B4 purified without detergent removal also had a Soret band at 390 nm, typical of high-spin ferric haem iron [13], but Noordermeer et al. [13] could not detect any such iron by EPR due to a temperature 'dependency' of the EPR signals. Psylinakis et al. [24], studying CYP74B1, suggested that there was no such 'dependency', as they could detect high-spin ferric haem iron by EPR, and that the inability to detect such iron in CYP74B4 may have been due to contamination with imidazole that was used by Noordermeer et al. [13] in their purification. In the present study, with CYP74C3, histidine was used instead of imidazole during the purification, and there was complete agreement on spin state of the haem iron using both UV–visible and EPR data, suggesting no temperature dependency. The loss of intensity in the EPR signals observed after reaction of CYP74C3 (in the presence and absence of detergent micelles) with 13-HPOTE was most likely explained by the formation of an EPR silent intermediate(s) during turnover because: (i) there was no evidence of haem dissociation or enzyme inactivation, (ii) no new features in the EPR spectra were seen at 10 and 45 K, (iii) no changes could be detected in the redox state of the haem iron, and (iv) there was no evidence of any haem–haem interactions as a result of some change in oligomerization. The effects on the UV–visible spectrum of adding detergent micelles to detergent-free CYP74C3 were very similar to those observed for CYP1A2 [53] or CYP2B4 [54] (see Supplementary Table 2 at http://www.BiochemJ.org/bj/395/bj3950641add.htm). In the presence of 10 mM n-octyl glucoside, a complete loss of catalytic activity and a shift to low-spin haem iron of CYP2B4 with reductase was observed due to disaggregation of the active pentamer or hexamer into inactive monomers [14]. However, the effects of Emulphogene on CYP2B4 (and CYP1A2) activity appear to be more contradictory (see [55]), with reports of both loss of, and increases in, catalytic activity, due to the formation of monomers or dimers respectively. Certainly for the effects of Emulphogene on CYP74C3 in the present study, there was a positive correlation between the proportion of low-spin haem iron (determined by both UV–visible and EPR spectroscopy) and catalytic-centre activity. Our observations are not the first to demonstrate the effect of detergent micelles on improving the catalytic activity of CYP74 enzymes [29,48], but they are the first to explore the relationship between catalytic-centre activity and oligomeric state for this class of cytochrome P450 enzyme. Previously, it has only been speculated that the effect of detergent or high salt on increasing catalytic activity of an HPL was a result

of some conformational change in the protein [29]. To our knowledge, no studies in this regard have been carried out for an AOS.

CYP74C3 required extraction and purification in the presence of detergent, but unlike other HPLs, it remained soluble and active as a monomer when both detergent and salt were removed. The protein was almost entirely monomeric at concentrations from 0.5 to 15 mg/ml over a wide range of pH and ionic strengths. In the presence of detergent micelles, however, the most active CYP74C3 oligomer was of the size of a protein dimer, which is a new observation. This contrasts with other reports where HPL purified from higher plants was either a trimer or a tetramer [15–23]. In those instances where gel filtration was carried out in the presence of detergent and aggregation prevented, the higher molecular mass estimations may have been due to the formation of HPL complexes with the large (molecular mass 90 kDa) detergent micelles of Triton X-100 that was used at concentrations well above the c.m.c. (0.24 mM) of this detergent [40]. These HPLs may also have been considerably more hydrophobic than CYP74C3, which might explain their insolubility in the absence of detergent. In the present study, since Emulphogene was used at a concentration of 1.56 mM that is also well above the c.m.c. of this detergent (0.125 mM), micelles of average molecular mass 62.1 kDa would have formed under the conditions used for gel filtration. The identification of a CYP74C3 monomer and no dimer under detergent-free conditions was perhaps not surprising because any protein-bound detergent remaining would have been at concentrations well below the c.m.c., and the detergent would have been entirely monomeric. Any complex formation with protein and Emulphogene micelle would increase the molecular mass from 56.8 to 118.9 kDa, but no protein of this size or activity at this peak position in gel filtration under detergent-free conditions was detected. In contrast, in the presence of detergent buffer, the molecular mass of the most active species was the size of a protein dimer, or of a complex between a protein monomer and an Emulphogene micelle. The conclusion of dimer formation for CYP2B4 in the presence of detergent [55] was based on the results of gel filtration in the presence of Emulphogene, but like CYP74C3, may have corresponded to a protein monomer–micelle complex, rather than a protein dimer.

Regardless of the method of purification, CYP74C3 under the conditions of the activity assay was almost entirely monomeric. Nevertheless, the k_{cat} of the detergent-free monomer with the preferred substrate was only 10 % of the activity of the same enzyme in detergent buffer. It may be suggested that the low level of activity in the detergent-free preparation was due to contamination with a small amount of more active higher oligomer. However, clean separation of the monomer from the dimer by gel filtration on Superdex 75, and the presence of enzyme activity in only the fraction corresponding to the size of the monomer, suggests that this was unlikely. Under detergent-free conditions, the 10 % residual activity more likely resulted from CYP74C3 monomers, which may or may not have been contaminated with detergent monomers that coated hydrophobic patches on the surface of the protein. We propose that detergent-free monomers exhibited reduced substrate binding through a conformational change that was induced by release from a micellar or membrane environment. Complete re-activation of detergent-free CYP74C3 with the detergent Emulphogene was possible only at concentrations of at least 26-fold higher than the c.m.c., which suggested that detergent micelles (or the simulation of a membranous environment) and not monomers were required to maintain the most active conformation of CYP74C3. This evidence, together with the observation that the smallest and most active protein species detected by gel filtration in the presence of Emulphogene corresponded to the size of a monomer–micelle, suggested that an association between a protein monomer and a detergent micelle was the most active conformation for CYP74C3 and not a protein dimer. Further evidence for the lack of protein dimer formation comes from the absence, in concentrated detergent-free CYP74C3 preparations before and after re-activation with Emulphogene, of EPR signals corresponding to haem–haem interactions, and of protein sedimenting with the M_w of a dimer in the analytical ultracentrifuge. The small amount of protein dimer that was detected under detergent-free conditions in the analytical ultracentrifuge was shown not to be in reversible equilibrium with protein monomer. Increases in the activity and tightness of binding for CYP74C3 purified in detergent buffer were unexpected because the concentration of detergent present in the activity assay would have been well below the c.m.c. This must suggest that the interaction between detergent micelle and protein monomer was stable over the very short time course of the activity assay (20 s); the low K_d determined for micelle binding of only 6.9 μM certainly indicated that this association was very tight; indeed, it was tighter than that for the preferred substrate ($K_m = 20.9$ μM).

13-HPOTE is only sparingly soluble in aqueous solution so it is important to distinguish between the substrate being presented from aqueous solution and from a micelle or membrane. It may be suggested that detergent micelles, or the formation of mixed substrate and detergent micelles, could facilitate substrate binding without any requirement for a change in protein conformation. 13-HPOTE was, however, entirely monomeric and did not form any micelles under our experimental conditions, even in the presence of Emulphogene micelles. This suggested that re-activation of detergent-free CYP74C3 (and the observed changes in spin state of the haem iron) required either detergent micelles or substrate monomers, and that substrate presentation could not account for CYP74C3 re-activation.

We hypothesize that in *E. coli*, and most likely *in planta*, CYP74C3 is a peripheral membrane protein with small patches of hydrophobic surface residues that promote a tight association with membranes, most likely as monomers. Solubilization with detergents releases the monomers from the membranes and allows them to self-associate to form a mixture of monomer–micelles and higher oligomers through hydrophobic interaction. The nature of the hydrophobic domain of CYP74C3 that is necessary for membrane association in CYP74C3 is unknown. The N-terminal sequence of cytochrome P450 enzymes has been reported to be a membrane-binding domain [12], but the N-terminal sequence of CYP74C3 is not particularly hydrophobic and evidence from the present study suggests that it has no role in membrane binding. The structure of the engineered AOS domain from an AOS–LOX fusion chimaera was recently crystallized as a protein dimer [9], but this bears no similarity to CYP74C3. The present study would suggest that the association between a protein monomer and a single detergent micelle (or perhaps a phospholipid in a membrane), and not oligomeric state, regulates the catalytic activity of CYP74C3. This represents a new mechanism for a membrane-associated cytochrome P450 enzyme and may be a distinguishing feature of CYP74 enzymes that are distinct from classical cytochrome P450 enzymes that require association with a reductase in order to carry out their full range of biological activities.

Unlike other plant cytochrome P450 enzymes described so far, CYP74C3 is a natural variant that does not require protein engineering to improve water solubility. The detailed understanding of the physical and biochemical properties of CYP74C3 described in the present study has provided valuable information towards our understanding of the differences in reaction

mechanism of CYP74 and more typical cytochrome P450 enzymes and the first crystal or NMR solution structure for an HPL or other membrane-associated plant cytochrome P450 enzyme. The subsequent information that would be forthcoming on the primary determinants of substrate and product specificities, and an identification of the hydrophobic domain responsible for membrane association, are likely to be key requirements for the challenging aim of manipulating oxylipin metabolism *in planta*.

We thank the Samuel Roberts Noble Foundation (Ardmore, OK, U.S.A.) for providing the EST clone of CYP74C3, Professor Mats Hamberg for providing HPL substrates, Mr Guus van Zadelhoff and Professor Gerrit Veldink (University of Utrecht, The Netherlands) for help with the GC-MS analysis, and Drs Mike Naldrett, Igor Galetich and Miss Karen Wilson (Department of Biological Chemistry, John Innes Centre, Norwich, U.K.) for protein sequencing. This work was funded by a European Union-funded project 'Natural Oxylipins for Defence of Ornamentals (NODO)', project number QLK5-CT-2001-02445, and by the Biotechnology and Biological Sciences Research Council.

REFERENCES

1 Schoch, G. A., Attias, R., Belghazi, M., Dansette, P. M. and Werck-Reichhart, D. (2003) Engineering of a water-soluble plant cytochrome P450, CYP73A1, and NMR-based orientation of natural and alternate substrates in the active site. Plant Physiol. **133**, 1198–1208

2 Hasemann, C. A., Kurumbail, R. G., Boddupalli, S. S., Peterson, J. A. and Desienhofer, J. (1995) Structure and function of cytochromes P450: a comparative analysis of three crystal structures. Structure **2**, 41–62

3 Williams, P. A., Cosme, J., Sridhar, V., Johnson, E. F. and McRee, D. E. (2000) Mammalian microsomal cytochrome P450 monooxygenase: structural adaptations for membrane binding and functional diversity. Mol. Cell **5**, 121–131

4 Song, W.-C., Funk, C. D. and Brash, A. R. (1993) Molecular cloning of an allene oxide synthase: a cytochrome P450 specialised for the metabolism of fatty acid hydroperoxides. Proc. Natl. Acad. Sci. U.S.A. **90**, 8519–8523

5 Wang, L.-H., Tsai, A.-L. and Hsu, P.-Y. (2001) Substrate binding is the rate-limiting step in thromboxane synthase catalysis. J. Biol. Chem. **276**, 14737–14743

6 Grechkin, A. N., Mukhtarova, L. S. and Hamberg, M. (2003) Detection of an enol intermediate in the hydroperoxide lyase chain cleavage reaction. FEBS Lett. **549**, 31–34

7 Casey, R. and Hughes, R. K. (2004) Recombinant lipoxygenases and oxylipin metabolism in relation to food quality. Food Biotechnol. **18**, 135–170

8 Morant, M., Bak, S., Moller, B. L. and Werck-Reichhart, D. (2003) Plant cytochromes P450: tools for pharmacology, plant protection and phytoremediation. Curr. Opin. Biotechnol. **14**, 151–162

9 Oldham, M. L., Brash, A. R. and Newcomer, M. E. (2005) The structure of coral allene oxide synthase reveals a catalase adapted for metabolism of a fatty acid hydroperoxide. Proc. Natl. Acad. Sci. U.S.A. **102**, 297–302

10 Pan, Z., Camara, B., Gardner, H. W. and Backhaus, R. A. (1998) Aspirin inhibition and acetylation of the plant cytochrome P450, allene oxide synthase, resembles that of animal prostaglandin endoperoxide H synthase. J. Biol. Chem. **273**, 18139–18145

11 Mast, N., Andersson, U., Nakayama, K., Bjorkhem, I. and Pikulevaa, I. A. (2004) Expression of human cytochrome P450 46A1 in *Escherichia coli*: effects of N- and C-terminal modifications. Arch. Biochem. Biophys. **428**, 99–108

12 von Wachenfeldt, C., Richardson, T. H., Cosme, J. and Johnson, E. F. (1997) Microsomal P450 2C3 is expressed as a soluble dimer in *Escherichia coli* following modification of its N-terminus. Arch. Biochem. Biophys. **339**, 107–114

13 Noordermeer, M. A., van Dijken, A. J. H., Smeekens, S. C. M., Veldink, G. A. and Vliegenthart, J. F. G. (2000) Characterisation of three cloned and expressed 13-hydroperoxide lyase isoenzymes from alfalfa with unusual N-terminal sequences and different enzyme kinetics. Eur. J. Biochem. **267**, 2473–2482

14 Dean, W. L. and Gray, R. D. (1982) Relationship between state of aggregation and catalytic activity for cytochrome P-450LM2 and NADPH-cytochrome P-450 reductase. J. Biol. Chem. **257**, 14679–14685

15 Tijet, N., Waspi, U., Gaskin, D. J., Hunziker, P., Muller, B. L., Vulfson, E. N., Slusarenko, A., Brash, A. R. and Whitehead, I. M. (2000) Purification, molecular cloning, and expression of the gene encoding fatty acid 13-hydroperoxide lyase from guava fruit (*Psidium guajava*). Lipids **35**, 709–720

16 Shibata, Y., Matsui, K., Kajiwara, T. and Hatanaka, A. (1995) Purification and properties of fatty-acid hydroperoxide lyase from green bell pepper fruits. Plant Cell Physiol. **36**, 147–156

17 Husson, F. and Belin, J. M. (2002) Purification of hydroperoxide lyase from green bell pepper (*Capsicum annuum* L.) fruits for the generation of C6-aldehydes *in vitro*. J. Agric. Food Chem. **50**, 1991–1995

18 Itoh, A. and Vick, B. A. (1999) The purification and characterisation of fatty acid hydroperoxide lyase in sunflower. Biochim. Biophys. Acta **1436**, 531–540

19 Schreier, P. and Lorenz, G. (1982) Separation, partial-purification and characterisation of a fatty-acid hydroperoxide cleaving enzyme from apple and tomato fruits. Z. Naturforsch. **37**, 165–173

20 Fauconnier, M.-L., Perez, A. G., Sanz, C. and Marlier, M. (1997) Purification and characterisation of tomato leaf (*Lycopersicon esculentum* Mill.) hydroperoxide lyase. J. Agric. Food Chem. **45**, 4232–4236

21 Matsui, K., Miyahara, C., Wilkinson, J., Hiatt, B., Knauf, V. and Kajiwara, T. (2000) Fatty acid hydroperoxide lyase in tomato fruits: cloning and properties of a recombinant enzyme expressed in *Escherichia coli*. Biosci. Biotechnol. Biochem. **64**, 1189–1196

22 Olias, J. M., Rios, J. L., Valle, M., Zamora, R., Sartz, L. C. and Axelrod, B. (1990) Fatty-acid hydroperoxide lyase in germinating soybean seedlings. J. Agric. Food Chem. **38**, 624–630

23 Vick, B. A. and Zimmerman, D. C. (1976) Lipoxygenase and hydroperoxide lyase in germinating watermelon seedlings. Plant Physiol. **57**, 780–788

24 Psylinakis, E., Davoras, E. M., Ioannidis, N., Trikeriotis, M., Petrouleas, V. and Ghanotakis, D. F. (2001) Isolation and spectroscopic characterisation of a recombinant bell pepper hydroperoxide lyase. Biochim. Biophys. Acta **1533**, 119–127

25 Kandzia, R., Stumpe, M., Berndt, E., Szalata, M., Matsui, K. and Feussner, I. (2003) On the specificity of lipid hydroperoxide fragmentation by fatty acid hydroperoxide lyase from *Arabidopsis thaliana*. J. Plant Physiol. **160**, 803–809

26 Howe, G. A., Lee, G. I., Itoh, A., Li, L. and DeRocher, A. E. (2000) Cytochrome P450-dependent metabolism of oxylipins in tomato. Cloning and expression of allene oxide synthase and fatty acid hydroperoxide lyase. Plant Physiol. **123**, 711–724

27 Matsui, K., Ujita, C., Fujimoto, S.-H., Wilkinson, J., Hiatt, B., Knauf, V., Kajiwara, T. and Feussner, I. (2000) Fatty acid 9- and 13-hydroperoxide lyases from cucumber. FEBS Lett. **481**, 183–188

28 Tijet, N., Schneider, C., Muller, B. L. and Brash, A. R. (2001) Biogenesis of volatile aldehydes from fatty acid hydroperoxides: molecular cloning of a hydroperoxide lyase (CYP74C) with specificity for both the 9- and 13-hydroperoxides of linoleic and linolenic acids. Arch. Biochem. Biophys. **386**, 281–289

29 Koeduka, T., Stumpe, M., Matsui, K., Kajiwara, T. and Feussner, I. (2003) Kinetics of barley FA hydroperoxide lyase are modulated by salts and detergents. Lipids **38**, 1167–1172

30 Scott, E. E., He, Y. A., Wester, M. R., White, M. A., Chin, C. C., Halpert, J. R., Johnson, E. F. and Stout, C. D. (2003) An open conformation of mammalian cytochrome P450 2B4 at 1.6-Å resolution. Proc. Natl. Acad. Sci. U.S.A. **100**, 13196–13201

31 Schoch, G. A., Yano, J. K., Wester, M. R., Griffin, C., Stout, E. F. and Johnson, E. F. (2004) Structure of human microsomal cytochrome P450 2C8: evidence for a peripheral fatty acid binding site. J. Biol. Chem. **279**, 9497–9503

32 Williams, P. A., Cosme, J., Ward, A., Angove, H. C., Vinkovic, D. M. and Jhoti, H. (2003) Crystal structure of human cytochrome P450 2C9 with bound warfarin. Nature (London) **424**, 464–468

33 Yano, J. K., Wester, M. R., Schoch, G. A., Griffin, K. J., Stout, C. D. and Johnson, E. F. (2004) The structure of human microsomal cytochrome P450 3A4 determined by X-ray crystallography to 2.05-A resolution. J. Biol. Chem. **279**, 38091–38094

34 Yano, J. K., Hsu, M. H., Griffin, K. J., Stout, C. D. and Johnson, E. F. (2005) Structures of human microsomal cytochrome P450 2A6 complexed with coumarin and methoxsalen. Nat. Struct. Mol. Biol. **12**, 822–823

35 Zhukovsky, E. A., Lee, J. O., Villegas, M., Chan, C., Chu, S. and Mroske, C. (2004) TNF ligands: is TALL-1 a trimer or a virus-like cluster? Nature (London) **427**, 413–414

36 Vick, B. A. (1991) A spectrophotometric assay for hydroperoxide lyase. Lipids **26**, 315–320

37 Aase, R. and Vanngard, T. (1975) EPR signal intensity and powder shapes – re-examination. J. Magn. Reson. **19**, 308–315

38 Berry, E. A. and Trumpower, B. (1987) Simultaneous determination of haems a, b, and c from pyridine haemochrome spectra. Anal. Biochem. **161**, 1–15

39 Bradford, M. M. (1976) A rapid and sensitive method for the quantitation of microgram quantities of protein utilizing the principle of protein–dye binding. Anal. Biochem. **72**, 248–254

40 Helenius, A. and Simons, K. (1975) Solubilisation of membranes by detergents. Biochim. Biophys. Acta **415**, 29–79

41 Noordermeer, M. A., Veldink, G. A. and Vliegenthart, J. F. G. (1999) Alfalfa contains substantial 9-hydroperoxide lyase activity and a 3*Z*:2*E*-enal isomerase. FEBS Lett. **443**, 201–204

42 Schuck, P. (2000) Size-distribution analysis of macromolecules by sedimentation velocity ultracentrifugation and lamm equation modelling. Biophys. J. **78**, 1606–1619

43 Colfen, H. and Harding, S. E. (1997) MSTARA and MSTARI: interactive PC algorithms for simple, model independent evaluation of sedimentation equilibrium data. Eur. Biophys. J. Biophys. Lett. **24**, 333–346
44 Laue, T. M., Shah, B. D., Ridgeway, T. M. and Pelletier, S. L. (1992) Computer-aided interpretation of analytical sedimentation data for proteins. In Analytical Ultracentrifugation in Biochemistry and Polymer Science (Harding, S. E., Rowe, A. J. and Horton, J. C., eds.), pp. 90–125, Royal Society of Chemistry, Cambridge, U.K.
45 Squire, P. G. and Himmel, M. E. (1979) Hydrodynamics and protein hydration. Arch. Biochem. Biophys. **196**, 165–177
46 Rahfeld, J.-U., Rucknagel, P., Stoller, G., Horne, S. M., Schierhorn, A., Young, K. D. and Fischer, G. (1996) Isolation and amino acid sequence of a new 22-kDa FKBP-like peptidyl-prolyl *cis*/*trans*-isomerase of *Escherichia coli*: similarity to Mip-like proteins of pathogenic bacteria. J. Biol. Chem. **271**, 22130–22138
47 Abraham, B. D., Sono, M., Boutaud, O., Shriner, A., Dawson, J. H., Brash, A. R. and Gaffney, B. J. (2001) Characterisation of the coral allene oxide synthase active site with UV-visible absorption, magnetic circular dichroism, and electron paramagnetic resonance spectroscopy: evidence for tyrosinate ligation to the ferric enzyme haem iron. Biochemistry **40**, 2251–2259
48 Song, W.-C. and Brash, A. R. (1991) Purification of an allene oxide synthase and identification of the enzyme as a cytochrome P-450. Science **253**, 781–784
49 Noordermeer, M. A., Veldink, G. A. and Vliegenthart, J. F. G. (2001) Spectroscopic studies on the active site of hydroperoxide lyase: the influence of detergents on its conformation. FEBS Lett. **489**, 229–232
50 White, R. E. and Coon, M. J. (1982) Haem ligand replacement reactions of cytochrome P-450. Characterisation of the bonding atom of the axial ligand trans to thiolate as oxygen. J. Biol. Chem. **257**, 3073–3083
51 Bordwell, F. G. (1988) Equilibrium acidities in dimethyl sulphoxide solution. Acc. Chem. Res. **21**, 456–463
52 Lindskog, S., Engberg, P., Forsman, C., Ibrahim, S. A., Johnson, B. H., Simosson, I. and Tibell, L. (1984) Kinetics and mechanism of carbonic anhydrase isoenzymes. Ann. N. Y. Acad. Sci. **429**, 61–75
53 Haugen, D. A. and Coon, M. J. (1976) Properties of electrophoretically homogeneous phenobarbital-inducible and beta-naphthoflavone-inducible forms of liver microsomal cytochrome P-450. J. Biol. Chem. **251**, 7929–7939
54 Wagner, S. L. and Gray, R. D. (1985) Effects of detergent on substrate binding and spin state of purified liver microsomal cytochrome P-450LM2 from phenobarbital-treated rabbits. Biochemistry **24**, 3809–3814
55 Viner, R. I., Novikov, K. N., Ritov, V. B., Kagan, V. E. and Alterman, M. A. (1995) Effect of different solubilizing agents on the aggregation state and catalytic activity of two purified rabbit cytochrome P450 isozymes, CYP1A2 (LM4) and CYP2B4 (LM2). Biochem. Biophys. Res. Commun. **217**, 886–891

Received 14 October 2005/26 January 2006; accepted 2 February 2006
Published as BJ Immediate Publication 2 February 2006, doi:10.1042/BJ20051667